Function of Tyrosine Z in Water Oxidation by Photosystem II: Electrostatical Promotor Instead of Hydrogen Abstractor[†]

Ralf Ahlbrink,[‡] Michael Haumann,[‡] Dmitry Cherepanov,[§] Oliver Bögershausen,[‡] Armen Mulkidjanian,[‡,||] and Wolfgang Junge*,[‡]

Abt. Biophysik, FB. Biologie/Chemie, Universität Osnabrück, D-49069 Osnabrück, Germany, A. N. Frumkin Institute of Electrochemisty, Russian Academy of Sciences, Moscow 117071, Russia, and A. N. Belozersky Institute of Physico-Chemical Biology, Moscow State University, Moscow 118899, Russia

ABSTRACT: Photosynthetic water oxidation by photosystem II is mediated by a Mn_4 cluster, a cofactor X still chemically ill-defined, and a tyrosine, Y_Z (D1-Tyr161). Before the final reaction with water proceeds to yield O_2 (transition $S_4 \rightarrow S_0$), two oxidizing equivalents are stored on Mn_4 ($S_0 \rightleftharpoons S_1 \rightleftharpoons S_2$), a third on X ($S_2 \rightleftharpoons S_3$), and a forth on Y_Z ($S_3 \rightleftharpoons S_4$). It has been proposed that Y_Z functions as a pure electron transmitter between Mn_4X and P_{680}, or, more recently, that it acts as an abstractor of hydrogen from bound water. We scrutinized the coupling of electron and proton transfer during the oxidation of Y_Z in PSII core particles with intact or impaired oxygen-evolving capacity. The rates of electron transfer to P_{680}^+, of electrochromism, and of pH transients were determined as a function of the pH, the temperature, and the H/D ratio. In oxygen-evolving material, we found only evidence for electrostatically induced proton release from peripheral amino acid residues but not from Y_Z^{ox} itself. The positive charge stayed near Y_Z^{ox}, and the rate of electron transfer was nearly independent of the pH. In core particles with an impaired Mn_4 cluster, on the other hand, the rate of the electron transfer became strictly dependent on the protonation state of a single base ($pK \approx 7$). At pH <7, the rate of electron transfer revealed the same slow rate ($t_{1/2} \approx 35 \mu s$) as that of proton release into the bulk. The deposition of a positive charge around Y_Z^{ox} was no longer detected. A large H/D isotope effect (≈ 2.5) on these rates was also indicative of a steering of electron abstraction by proton transfer. That Y_Z^{ox} was deprotonated into the bulk in inactive but not in oxygen-evolving material argues against the proposed role of Y_Z^{ox} as an acceptor of hydrogen from water. Instead, the positive charge in its vicinity may shift the equilibrium from bound water to bound peroxide upon $S_3 \rightleftharpoons S_4$ as a prerequisite for the formation of oxygen upon $S_4 \rightarrow S_0$.

Photosystem II of higher plants and cyanobacteria is a multisubunit protein−pigment complex which oxidizes two molecules of water and produces dioxygen at the expense of four quanta of light (*1−3*). After photo-oxidation of the primary electron donor P_{680}[1] (which is presumably a specialized chlorophyll *a* dimer that is located close to the lumenal side of the thylakoid membrane), the electron vacancy on

P_{680}^+ is filled in nanoseconds (*4, 5*) by an electron from a redox-active tyrosine, Y_Z [D1-Tyr161 (*6−8*)]. The latter is in turn reduced in micro- to milliseconds by the oxygen-evolving complex (OEC) that catalyzes the oxidation of water (*9*). It contains four manganese atoms [Mn_4 (*10, 11*)], probably a further redox cofactor, X, whose chemical nature is still ill-defined (*12−14*), and Ca^{2+} and Cl^- ions (*2, 15*). Clocked by four quanta of light, the OEC cycles through the increasingly oxidized states $S_0 \rightleftharpoons S_1 \rightleftharpoons S_2 \rightleftharpoons S_3 \rightleftharpoons S_4 \rightarrow S_0$. The release of dioxygen is associated with the last transition $S_4 \rightarrow S_0$, which spontaneously advances in the dark (*16*).

Y_Z and its counterpart Y_D (D2-Tyr161) have been proposed to be located at a distance of 10−15 Å from P_{680} (*17−19*), in positions that correspond to residues L-Arg135 and M-Arg162 on the L and M subunits of the bacterial reaction center (BRC) (*20−22*). The electrogenicity of the electron transfer from Y_Z to P_{680}^+ (*23−26*) and data on local electrochromic band shifts in PSII (*27*) are compatible with this notion.

The distance between the Mn cluster and Y_Z is under debate. On the basis of EPR, some authors have claimed

* Corresponding author. Telephone: ++49-541-9692872. Fax: ++49-541-9691221. E-mail: JUNGE@UNI-OSNABRUECK.DE.
[‡] Universität Osnabrück.
[§] Russian Academy of Sciences.
[||] Moscow State University.

[1] Abbreviations: A and B, acid/base residues; Bis-Tris, bis(2-hydroxyethyl)iminotris(hydroxymethyl)methane; BRC, bacterial reaction center; β-DM, *n*-dodecyl β-D-maltoside; cw, continuous wave; DCBQ, 2,5-dichloro-*p*-benzoquinone; E_m, midpoint redox potential; ENDOR, electron nuclear double resonance; EPR, electron paramagnetic resonance; Mes, 2-*N*-morpholinoethanesulfonic acid; Mn_4X, redox cofactors of the OEC; NHE, normal hydrogen electrode; OEC, oxygen-evolving complex; PSII, photosystem II; P_{680}, primary donor in photosystem II; Q_A and Q_B, primary and secondary electron acceptor quinones, respectively; X, chemically undefined cofactor; Y_Z and Y_D, tyrosines 161 on subunits D1 and D2 of PSII.

that Y_Z is relatively far away from Mn, at a distance of 8−20 Å (*17, 28−30*). Correspondingly, Y_Z has not been said to be directly involved in a reaction with water but just as an electron transfer component in the consecutive sequence of redox reactions water → manganese → Y_Z → P_{680}. Contrastingly, a much smaller distance between Y_Z and Mn of only 4.5 Å has recently been inferred on the basis of ENDOR data (*31, 32*), and these and other data (see below) have been interpreted to show a more direct involvement of Y_Z in the water chemistry. On the basis of the observation that the hydrogen bonds to Y_Z^{ox} were found to be less ordered than those of Y_D^{ox} (*31, 33−36*), and that the rotational mobility of Y_Z^{ox} was slightly larger (*34, 37*) in calcium-depleted PSII, it has been hypothesized that the oxidized Y_Z rapidly releases its hydroxyl proton into bulk water to serve as an abstractor of hydrogen from bound water (*32, 38−40*). These data were, however, obtained on material with impaired oxygen evolution. It is thus an open question of whether Y_Z serves as (a) an electron acceptor or (b) an abstractor of hydrogen from bound water. We have previously argued in favor of an electron acceptor function of Y_Z because of the detectable charge around it and the lack of detectable proton release into the bulk from Y_Z^{ox} (*41, 42*). The fact that we have reported rapid proton release [at rise times down to 10 μs (*43, 44*)] has been misinterpreted by some authors as a deprotonation of Y_Z into the bulk. This has prompted us to carry out this detailed study.

We analyzed the reactions involving Y_Z in a systematic way, both in fully functional and in inactive (Mn-depleted) core particles. We measured the rate of electron transfer from Y_Z to P_{680}^+, the release of protons and electrochromic band shifts of intrinsic pigments as a function of the pH, of the isotopic ratio of H_2O/D_2O, and of the temperature. The results give clues for solving the seeming incompatibility of two observations from the literature, namely the status of Y_Z^{ox} as an electroneutral radical (*45*) and the lack of detectable proton release together with the large electrochromism (*41*) that is caused by Y_Z^{ox}. We consider two equally possible solutions. (1) Y_Z^{ox} is a $Y_Z^{\bullet}\cdots H^+$-B^- pair wherein B^- denotes a base in close vicinity to Y_Z. (2) Y_Z is in the anionic form (Y_Z^-) under physiological conditions, and it is oxidized to the neutral $Y_Z^{\bullet}$. In both cases the oxidized Y_Z is hardly appropriate as an acceptor of hydrogen from water.

MATERIALS AND METHODS

Oxygen-evolving PSII core particles were prepared from 12-day-old pea seedlings according to van Leeuwen et al. (*46*) with modifications as in ref 44. Concentrated core particles were stored at −80 °C in 20 mM Bis-Tris/HCl, 400 mM sucrose, 20 mM $MgCl_2$, 5 mM $CaCl_2$, 10 mM $MgSO_4$, and 0.03% (w/v) β-DM at pH 6.5 until use. For one experiment, we used PSII core particles prepared according to ref 47. They were stored in 20 mM MES, 400 mM sucrose, and 10 mM $CaCl_2$ at pH 6.5. After thawing, core particles were suspended in 5 μM chlorophyll (except for measurements at 827 nm, see below), 5 mM $CaCl_2$, 5 mM $MgCl_2$, and 20 mM buffer (pH 4−7, MES; pH 6−8, Bis-Tris; pH 7−8, Tricine; and pH 8−11, Tris). The buffers were omitted in experiments on pH transients.

Inactivation of core particles was achieved by pH 9 treatment. A suspension with 5 μM chlorophyll was titrated to pH 9 for 5 min, and then the pH was readjusted to the desired value directly before the measurements. Oxygen evolution was below 10% of a control after this treatment. It should be noted that the behavior of samples treated at pH 9 in flash-spectroscopic measurements was indistinguishable from that of samples that were depleted of manganese by the classical Tris-wash treatment (*48, 49*). The pH 9 treatment thus probably also resulted in the release of Mn from its binding site (*50*).

The substitution of D_2O for H_2O was performed as follows. After thawing, the PSII-containing material was suspended in a medium with D_2O (99.7% pure), at pL 6.5 (L = lyonium ion, H or D) and at the final chlorophyll concentrations for the measurements. Samples were then incubated in the light (2 mW cm^{-2}) for 5 min at room temperature and, after readjusting the pL to the desired value, dark-adapted for 15 min prior to the first flash train. It should be noted that the maximum H/D isotope effects were already achieved after a much shorter incubation time, e.g. less than 1 min, as is apparent from measurements of absorption changes at 827 nm as a function of the incubation interval (data not documented).

The reduction of P_{680}^+ was measured as flash-induced absorption changes at 827 nm (*13*). The beam of a stabilized cw laser diode was focused through a 5 cm long cuvette and a pinhole at a distance of about 1 m on a fast avalanche photodiode. This setup suppressed the fluorescence of the sample and scattered light. A Q-switched, frequency-doubled Nd:YAG laser served as the excitation source (flash duration of 6 ns, 532 nm). The maximal electrical bandwidth of the system was dc to 150 MHz (4 ns per address). Transients were digitized and averaged for signal-to-noise improvement on a Tektronix DSA602 recorder. Samples contained 50 μM chlorophyll and 1 mM hexacyanoferrate-(III) plus 0.5 mM DCBQ as electron acceptors. Samples of PSII core particles with impaired oxygen evolution also contained 0.5 mM hexacyanoferrate(II) as electron donor. Under these conditions, Q_A^- was stable for at least 5 ms at pH 8.

Flash spectrophotometry at wavelengths other than 827 nm was performed with the setup described in ref *51*. A xenon flash lamp (flash duration of 10 μs) was used for excitation. The optical path length was 1 cm. The maximal electrical bandwidth of the system was 100 kHz (5 μs per address). Transients were digitized and averaged on a Nicolet Pro30 recorder. For the electron acceptor conditions of the samples, see the legends to the figures.

Proton release was measured with various pH-indicating dyes at 30 μM (pH 4.5−6, methyl red at 548 nm; pH 5−7, bromocresol purple at 575 nm; and pH 6.5−8.5, phenol red at 559 nm) (*44*). From transients in the presence of the dyes, background transients obtained under the same conditions but in the further presence of 20 mM buffer were subtracted.

Local electrochromism due to Y_Z^{ox} was recorded at 443 nm as previously described (*52*).

Oxygen evolution was measured under continuous white light illumination with a Clark-type electrode with 4 μM chlorophyll at 20 °C with 500 μM DCBQ as an electron acceptor.

The time course of absorption transients was analyzed in terms of exponentials using commercial routines.
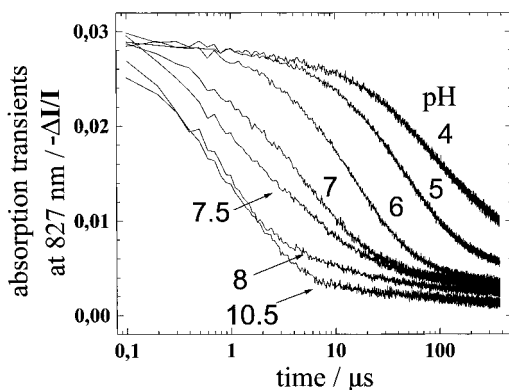
FIGURE 1: Flash-induced absorption transients at 827 nm indicating the reduction of P_{680}^+ at pH values ranging from 4 to 10.5 in inactive PSII core particles. A logarithmic time scale was chosen to display the full decay of the transients. The time resolution was 100 ns per address; 50 transients were averaged for each trace, and the samples were repetitively excited every 5 s.

RESULTS

Rate of Oxidation of Y_Z in Photosystem II with Impaired Oxygen Evolution

Influence of pH. Oxygen evolution by PSII core particles was inactivated by incubation at pH 9 (see Materials and Methods). Electron transfer from Y_Z to P_{680}^+ was monitored at 827 nm. Absorption transients at this wavelength can be attributed to the radical cation P_{680}^+ (*53–56*). Figure 1 shows raw transients due to the oxidation/reduction of P_{680} in the time interval from 100 ns to 100 μs after the first exciting flash at six pH values ranging from pH 4 to 10.5 (note the logarithmic time scale). The overall decay time of P_{680}^+ was strongly pH-dependent; it decreased from about 200 μs at pH 4 to 1 μs at pH >8. The major portion of the pH-dependent decay could be attributed to electron transfer to P_{680}^+ from Y_Z. Our data are in line with other data obtained on Tris-washed PSII (*49, 57, 58*). The approximation of the decay of P_{680}^+ in Figure 1 by a single exponential was rather poor. Three exponents were more appropriate, according to

$$\Delta A(t) = a_f e^{-k_f t} + a_s e^{-k_s t} + a_v e^{-k_v t} \qquad (1)$$

wherein a_f, a_s, and a_v, and k_f, k_s, and k_v correspond to the extents and rates of the fast, slow, and very slow components, respectively. Figure 2A (top) shows the pH dependence of the respective rate constants of the fast (k_f, squares) and the slow component (k_s, circles) over a wide pH range from 4 to 10. Figure 2B (middle) shows the respective extents, and Figure 2C (bottom) shows the extent of the very slow component (k_v, open triangles).

k_f was little dependent on the pH, and between 6 and 10.5, it averaged to 7×10^5 s^{-1} which is equivalent to a half-decay time of about 1 μs. k_s, on the other hand, decreased by a factor of 5 from 10^5 s^{-1} ($t_{1/2} = 7$ μs) at pH 8 to about 2×10^4 s^{-1} ($t_{1/2} = 35$ μs) at pH 4.

The extents of the fast and the slow kinetic components were pH-dependent. They are shown in Figure 2B. At pH >7, the fast component (squares) was dominant with an amplitude of about 80% at pH 10. Its relative extent decreased to about 10% at pH 5.5 with an apparent pK of 7 (line). The slow component (Figure 2B, circles) prevailed
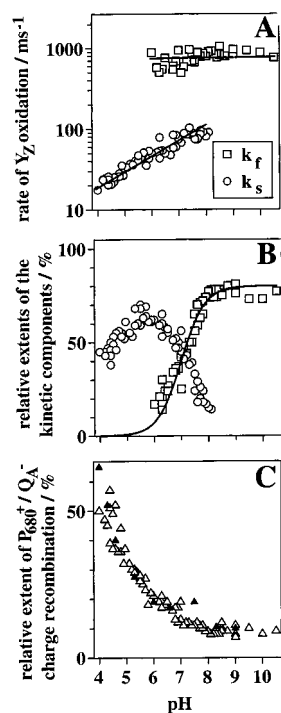
FIGURE 2: Rates and extents of the kinetic components of the reduction of P_{680}^+ in inactive PSII core particles as a function of the pH. (A) The rates of the two faster kinetic components from a fit of transients as in Figure 1 by three exponentials plus an offset. The rate of the fastest component (k_f, □) was about pH-independent (—), whereas the rate of the slower one (k_s, ○) decreased with the pH (—). (B) The relative extents of the two kinetic components (k_f, □; k_s, ○) from panel A. The extents of k_f (□) were described by a single titration with a pK of 7 (—). For details, see the text. (C) The sum of the extents of the very slow components (k_v) as a function of the pH: (△) data from absorption transients at 827 nm which reflected the oxidoreduction of P_{680} and (▲) data from transients at 320 nm which reflected the oxidoreduction of Q_A.

at pH <7. Its amplitude increased from about 10% at pH 8 to 70% at pH 5.5, and again decreased below pH 5.5. The increase of the amplitude of the slow component thus occurred at the expense of the extent of the fast component, again with an apparent pK of 7.

At pH <6, an additional very slow component (k_v) rose up. Its total extent increased to about 60% at pH 4 (Figure 2C, open triangles). Its average rate constant (k_v) was about 1500 s^{-1} (half-decay time of 450 μs). We suspected that the very slow component could be attributed to the recombination of the charge pair P_{680}^+/Q_A^-. To test this possibility, we directly monitored the reoxidation of Q_A^- at 320 nm where the quinone anion strongly absorbs (*59–61*). The upper part of Figure 3 shows UV transients at pH values ranging between 4 and 9 on the first flash given to inactive centers. At pH 9, the decay was rather slow and due to oxidation of Q_A^- by external acceptors. It speeded up at more acidic pH. The bottom trace in Figure 3 shows the difference between transients obtained at pH 9 minus 4. The overall half-decay time of the difference signal was 450 μs. It was coincident (Figure 2C, solid triangles) with the one determined for the very slow component of the reduction of P_{680}^+ (Figure 2C, open triangles; see also ref 62). The coincidence supports the notion that the latter could be attributed to the charge pair recombination between P_{680}^+ and Q_A^-. A fit of the difference transient in Figure 3 by two exponentials (see the solid line) revealed two compo-

Table 1: Parameters of Electron Transfer, Proton Release, and Local Electrochromism in Inactive and Oxygen-Evolving PSII Core Particles[a]

	inactive PSII core particles			active PSII core particles	
	pH 8.0	pH 5.0	pH 4.0	pH 6.5	
	$Y_Z \rightarrow P_{680}^+$		$P_{680}^+ \leftarrow Q_A^-$	$Y_Z \rightarrow P_{680}^+$	
kinetic component	fast, k_f	slow, k_s	very slow, k_v	first flash (ns)	third flash (ns)
			Electron Transfer		
half-time (μs)	1	35	135/870	0.02	0.04/0.25
relative extent	0.8	0.6	0.3/0.3	0.65	0.3/0.4
H/D isotope effect	≤ 1.1	2.5	≤ 1.5	≤ 1.1	≤ 1.1
activation energy (eV)	0.15	0.30	≤ 0.10	≤ 0.10[b]	≤ 0.10[b]
apparent pK		7	–		4.5
			Proton Release		
half-time (μs)	450	40	–	85	
H/D isotope effect	1.6	4.0	–	2.5	
			Local Electrochromic Effect of Y_Z^{ox}		
relative extent	45	0	–	100	
apparent pK		7 (6[c])	–	4.5[d]	

[a] ns, nanosecond electron transfer in oxygen-evolving centers (see the text). [b] Data from ref *90*. [c] In core particles of the Ghanotakis/Lübbers type. [d] Data from ref *69*.
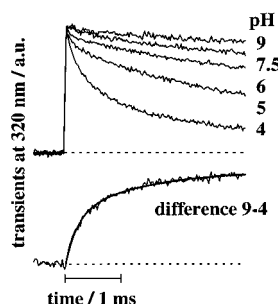
FIGURE 3: Flash-induced absorption transients at 320 nm in inactive PSII core particles due to the oxidation (rise) and reduction (decay) of Q_A: upper traces, at pH values ranging from 4 to 9; and lower traces, difference of transients at pH 9 minus 4. Measuring conditions: 5 μM chlorophyll, 100 μM DCBQ, 100 μM hexacyanoferrate(III), a time resolution of 5 μs per address, 50 transients averaged, and flash excitation every 10 s.

nents of equal extent with half-rise times of 135 and 870 μs (see Table 1). Taken together, the results which are documented in Figures 2 and 3 and Table 1 showed that the contribution of the charge recombination to the reduction of P_{680}^+ was negligible between pH 6 and 10, whereas it rose up to about 60−70% at pH 4. Forward electron transfer from Y_Z to P_{680}^+ was, however, still well separated from the charge recombination reaction because the former was at least 4 times faster than the latter even at the lowest pH values.

We summarized the rates of electron transfer between Q_A, P_{680}, and Y_Z in Table 1.

Effect of Temperature. We measured the influence of temperature on the rate of electron transfer from Y_Z to P_{680}^+ at pH 5 and 9. At pH 5 mainly the slow kinetic component (k_s) prevailed (relative extent of 65%) and at pH 9 the fast one (k_f, relative extent of 80%, compare Figure 2B). Figure 4 shows Arrhenius-type plots of k_f (squares) and k_s (circles) as a function of the temperature. The fast component revealed a small activation energy of 0.15 eV (pH 9, Table 1). The slow component (k_s) revealed a greater one, 0.30 eV (at pH 5, Table 1). A biphasic deconvolution of the kinetic traces at pH 6.3 yielded similar activation energies for the slow and fast components, namely 0.28 and 0.16 eV, respectively (dotted lines in Figure 4). At pH 4.0, the very
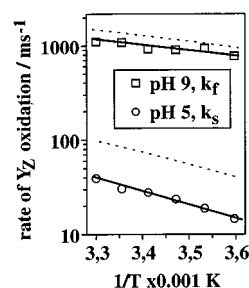
FIGURE 4: Arrhenius-type plot of the rates of electron transfer from Y_Z to P_{680}^+ in inactive PSII: fast component, k_f ($\square$), at pH 9; and slow component, k_s ($\bigcirc$), at pH 5. The dotted lines result from a biexponential fit of transients at pH 6.3.
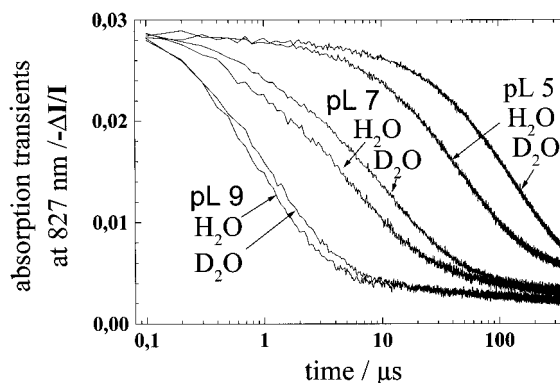
FIGURE 5: Comparison of flash-induced absorption transients at 827 nm at three pL values in H_2O and D_2O in inactive core particles. The measuring conditions were as in Figure 1.

slow components (k_v) that are due to charge pair recombination (see Figure 2C) revealed an even weaker temperature dependence (data not shown) which corresponded to an activation energy of ≤ 0.1 eV.

H/D Isotopic Substitution. We studied the effect of protium/deuterium substitution on the rate of Y_Z oxidation. This parameter was again studied at pH 5 and 9 where the slow and fast components prevailed. Figure 5 shows raw transients at 827 nm at these pH values as measured in H_2O and D_2O. We found that k_f was essentially independent on the substitution of D_2O against H_2O. The H/D isotope effect was less then 1.1 (Table 1). The slow component k_s, on the
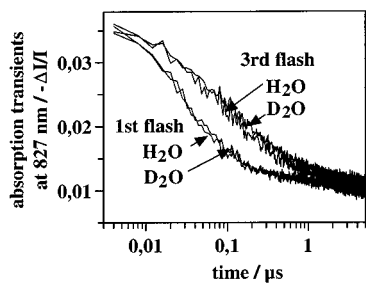
FIGURE 6: Flash-induced absorption transients at 827 nm in oxygen-evolving PSII core particles at pL 6.5 in H_2O and D_2O on the first and third flash given to dark-adapted samples. The time resolution was 4 ns per address; three flashes every 10 s; 50 cycles were averaged.

other hand, was substantially retarded in D_2O. Its H/D isotope effect was 2.5 at pL values between 7 and 5 (Table 1; see also ref 63). Charge recombination as observed at pL <5 (prevailing k_v) was apparently insensitive for isotopic substitution (data not shown).

Rate of Oxidation of Y_Z in Oxygen-Evolving Centers

Figure 6 shows transients at 827 nm due to the oxidation of P_{680}^+ on the first and third flash given to dark-adapted active centers at pL 6.5 in either H_2O or D_2O. The reduction of P_{680}^+ was multiphasic, and it occurred mainly in the nanosecond time range. Similar rates were observed on transitions $S_0 \Rightarrow S_1$ and $S_1 \Rightarrow S_2$ on one hand and on $S_2 \Rightarrow S_3$ and $S_3 \Rightarrow S_4$ on the other (Table 1). The former rates were greater than the latter (Table 1), in agreement with previous reports (*5, 64−66*). This behavior has been attributed to one extra positive charge on the Mn cluster which was brought in on transition $S_1 \Rightarrow S_2$ (see refs *5* and *67* and below). It was observed between pH 5.5 and 7. In this pH region, the oxygen-evolving capacity of the centers was about constant (compare Figure 10). Below pH 5, the nanosecond components were largely replaced by microsecond components which was accompanied by the reversible inactivation of oxygen evolution (see Figure 10), in line with previous reports (*68, 69*). An irreversible inactivation was also observed above pH 7.5, presumably due to the release of Mn (*50*). The nanosecond components were practically independent of H/D substitution; their isotope effect was less than 1.1 (Figure 6 and Table 1). That they were only weakly dependent on temperature between 35 and 0 °C (see Table 1) was in line with a previous report (*70*). Table 1 summarizes relevant data from the literature together with our results on the rate of Y_Z oxidation in intact PSII core particles.

By analyzing the equilibrium portion of P_{680}^+ (e.g. after nanosecond electron transfer was completed; see Table 1), we calculated the difference ΔE_i between the redox potentials $E_m(P_{680}^+/P_{680})$ and $E_m(Y_Z^{ox}/Y_Z)$ in the states S_0 and S_1 and S_2 and S_3, respectively, thus in the presence of zero ($i = 0$) and one ($i = 1$) positive net charge on the Mn cluster.

$$\Delta E_i = \frac{2.3RT}{F} \log \frac{[P_{680}]_{red}}{[P_{680}]_{ox}} \quad (2)$$

On the first flash, the equilibrium proportion of P_{680}^+ was only 5−10% (see ref *71* and this work). The calculated midpoint potential of P_{680} was by 80 mV more positive than
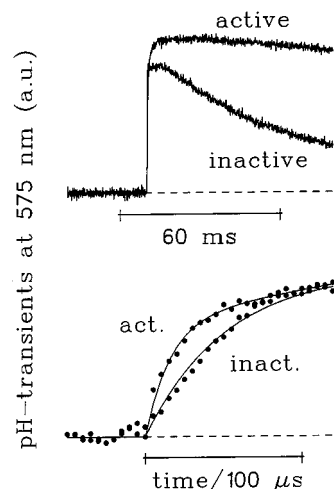
FIGURE 7: pH-indicating transients of bromocresol purple (30 μM) at 575 nm: active, on the first flash given to dark-adapted, oxygen-evolving PSII core particles; and inactive, repetitive excitation (every 30 s) of inactive core particles. Measuring conditions: 100 μM DCBQ, 100 μM hexacyanoferrate(III), 5 μM chlorophyll, 0.03% w/v β-DM, and 20 transients averaged at a time resolution of 5 μs per address. The lower traces show the upper ones on an expanded time scale.

that of Y_Z. Upon the second (and third) flash, about 20−25% of P_{680}^+ remained oxidized. This implied an initial energy gap of only 30 mV. Thus, the positive charge stored on the Mn cluster upon $S_1 \Rightarrow S_2$ increased the redox potential of Y_Z relative to P_{680} by a surprisingly low figure of only 50 mV.

Proton Release upon the Oxidation of Y_Z

In oxygen-evolving PSII the oxidation of Y_Z is accompanied by fast proton release in both thylakoids (*43, 72*) and core particles (*44*). We have previously proposed that the variability of the extent of proton release as a function of the pH (*43, 73−75*) and of the preparation (*47, 52, 74, 76*) argues against the notion that it originates from the phenolic moiety of Y_Z itself [pK of Y_Z^{ox} < −2 (*77*)]. This argument was corroborated by the pH dependence of the rate of proton release (*44*), showing its origin from electrostatically induced pK shifts of peripheral amino acids (for reviews, see refs *41* and *78*).

We compared the rates of proton release as monitored by pH-indicating dyes in inactive core particles with those in active core particles. The upper traces in Figure 7 represent pH-indicating transients of bromocresol purple at pH 5.3 upon a first flash given to dark-adapted centers. In active centers, the transient due to proton release upon the oxidation of Y_Z (Figure 7, rise) persisted for several hundred milliseconds. In inactive centers, on the other hand, the proton was released (rise) and rebound (decay) with a half-time of about 40 ms. This half-time was shortened when hexacyanoferrate(II) was added as an external donor for Y_Z^{ox} as previously reported (not shown here; see ref *13*). We interpreted these findings to be in line with our previous results (*42*). (1) In oxygen-evolving centers, the oxidation of Y_Z creates a positive net charge in the catalytic center that causes a pK shift of peripheral amino acids. The pK shift persists independent of the position of this net charge on Y_Z^{ox} or on the Mn cluster. This interpretation is backed up by extensive studies on the kinetics of proton release (*42−*
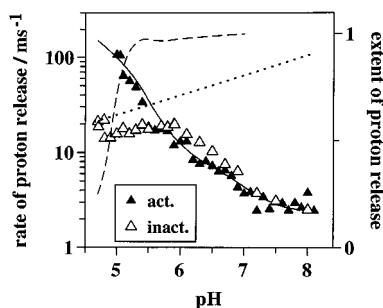
FIGURE 8: Rates of proton release (left coordinate scale) in inactive and oxygen-evolving PSII core particles as function of the pH: (▲) oxygen-evolving material and (△) inactive material. The dotted line shows the rates of the slow (k_s) component of electron transfer from Y_Z to P_{680}^+ in inactive centers for comparison. The solid line was calculated for the contributions of three peripheral acid groups to proton release with different pK values (see the text). The dashed line represents the extents of proton release per PSII center (right coordinate scale) in inactive core particles.

44), and by studies on local (*52, 79*) and transmembrane (*26*) electrochromism. (2) In inactive centers, the proton which is released upon the formation of Y_Z^{ox} is rebound when the latter is re-reduced (for a description of this push-and-pull mechanism of proton release/uptake, see refs *80–82*)). The lower traces in Figure 7 show the upper pH transients on an expanded time scale. In oxygen-evolving material, proton release occurred much faster at pH 5.3, with a half-time of about 15 μs, than in inactive centers where the half-time was about 40 μs (Table 1).

In Figure 8, we compared the rates of proton release in oxygen-evolving material (solid triangles, data replotted from ref *44*) and in inactive centers (open triangles) as a function of the pH. The rate of the slow kinetic component of electron transfer from Y_Z to P_{680}^+ in inactive material was replotted from Figure 2 for comparison (k_s, dotted line). In active centers, the rate of proton release decreased steeply between pH 5 and 7 and less steeply up to pH 8. This behavior can be rationalized by the participation of various peripheral amino acids with different pKs depending on the chosen pH in the medium (*44*). The rate of proton release from each group depends linearly on its pK (*44*), and the overall rate of the total release comprises the individual contributions of the various groups. The smooth line in Figure 8 was calculated for the simultaneous contributions of three groups with pK values of 7.5, 6, and 4.5. It describes the rates of proton release from active centers fairly well. In inactive centers and between pH 8 and 6, the rate of proton release was similar to that in active material. This result likely indicates that the same peripheral groups contributed to proton release in both materials at pH >6. At pH <6, the rate of proton release in inactive centers was lower than that in active centers and invariant, about 2×10^4 s^{-1} (35 μs). This rate was about the same as that of the main component (k_s) of the electron transfer from Y_Z to P_{680}^+.

There are two alternative interpretations for the lower rates of proton release in inactive centers at acidic pH (Figure 8). (a) Inactive centers may have lost some peripheral groups whose acid pKs give rise to the fastest proton release at acidic pH. (b) The release of protons in inactive centers may be limited by the rate of electron transfer or vice versa. Possibility (a) implied that the ratio of protons over electrons decreased below pH 6 in inactive centers. Such a decrease

was, however, not observed (Figure 8, dashed line, right coordinate scale). Instead, the extent decreased only below pH 5, concomitant with the increase of charge pair recombination. Under these conditions, no protons were apparently released in the presence of P_{680}^+. These results indicated that possibility (b) was more likely.

We determined the rate of proton release in inactive centers in both H_2O and D_2O as a function of the pH (raw data not shown). At pH 8, the H/D isotope effect was 1.6. At pH 5, it was much greater, namely 4 (Table 1). Similar H/D effects were, however, observed in active centers. The variability of the H/D isotope effect as a function of the pH was compatible with the contributions of various peripheral acid groups. If the pK difference between the acid and water (p$K = -2$) decreases by 3 units, one expects an increase of the isotope effect by a factor of about 2 (*83*).

From these results, we draw the following conclusions. (1) In active centers and over the whole studied pH range, a proton which is liberated from Y_Z^{ox} itself remains inside the protein for at least 300 μs, i.e. until an electron is transferred to Y_Z^{ox} from Mn_4X. The observed rapid protons [which may appear slower (at alkaline pH) or faster (at acidic pH) than the reduction of Y_Z^{ox}] result from peripheral groups. (2) Only in inactive material and at pH <6 are the rates of proton release and of electron transfer from Y_Z to P_{680}^+ similar. Only under these conditions may the proton which appears in the medium originate from the phenolic moiety of Y_Z^{ox}.

Local Electrochromism in the Presence of Y_Z^{ox}

The positive charge on or near Y_Z^{ox} causes local electrochromic bandshifts of the inner pigments in both active and inactive PSII (*27, 79, 84–87*). This effect has been used to estimate the mutual orientations of pigments and cofactors (*27*). Figure 9 shows time-resolved transients of local electrochromism at 443 nm upon the oxidoreduction of Y_Z. In dark-adapted, active centers upon the first flash (left trace, pH 7), the amplitude of the initial fast rise is due to the electrochromic effect of the formation of Y_Z^{ox} in nanoseconds plus a contribution of a chemical transient from Q_A^- (*60*). The latter decays with a half-time of about 10 ms under the used electron acceptor conditions (see the legend to Figure 9 and ref *88*). We determined the relative amplitude that could be attributed to Q_A^- by adding 1 mM hexacyanoferrate(III) and monitoring the extent of the accelerated decay (half-time about 0.5 ms) due to the reoxidation of Q_A^- (data not shown). The resulting relative extent of Q_A^- was drawn as a dotted line in Figure 9. The remaining amplitude could be attributed to the local electrochromic effect of Y_Z^{ox}. In active centers (left), the latter extent decayed to about half its initial value (Figure 9, left) upon electron transfer from Mn to Y_Z^{ox} on transition $S_1 \Rightarrow S_2$ with a half-time of 80 μs (see also ref *42*). In inactive centers this situation was completely changed. At pH 8 (Figure 9, inactive pH 8), the charge pair Y_Z^{ox}/Q_A^- was formed in about 1 μs (compare Figure 2A). Whereas the relative extent due to Q_A^- was as in active centers (dotted line), the extent that could be attributed to the electrochromism in response to Y_Z^{ox} was about halved. At pH 6.5 (Figure 9, inactive pH 6.5), the latter extent was close to zero. At both pH values, no decay in microseconds of the electrochromic effect due to Y_Z^{ox} was
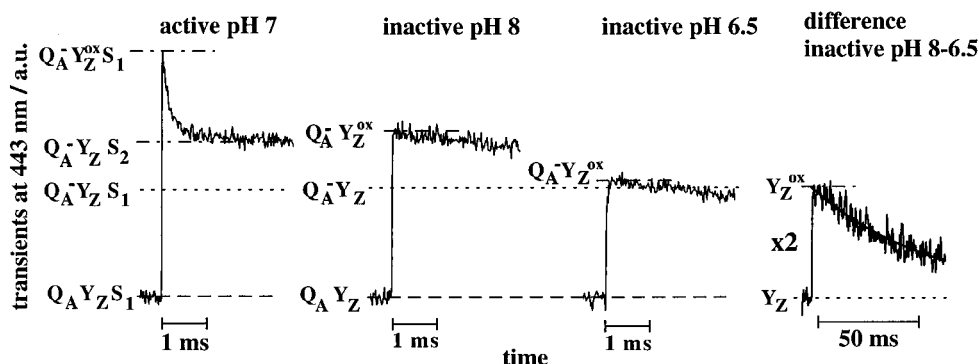
FIGURE 9: Flash-induced transients at 443 nm reflecting local electrochromic band shifts in PSII core particles: "active pH 7", oxygen-evolving centers, first flash given to dark-adapted samples; "inactive pH 8 and 6.5", inactive centers, repetitively excited every 30 s; "difference", difference of the two transients from inactive centers (the trace was scaled by a factor of 2 for comparison, and only every tenth point is shown). Note the longer time scale in the latter trace. Measuring conditions: 5 μM chlorophyll, 100 μM DCBQ, 100 μM hexacyanoferrate(III), and 20 transients averaged at a time resolution of 10 μs per address.
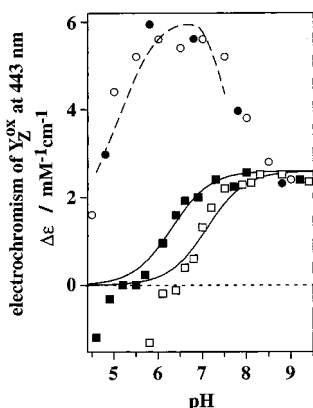
FIGURE 10: Extents of local electrochromism due to Y_Z^{ox} as a function of the pH: (open symbols) PSII core particles of the van Leeuwen/Bögershausen type, (solid symbols) core particles of the Ghanotakis/Lübbers type, (circles) oxygen-evolving samples, and (squares) inactive material. The solid lines correspond to single titrations with pK values of 7.1 and 6.1, respectively. The oxygen-evolving capacity is shown as a dashed curve for comparison; the maximum corresponds to about 1000 μmol of O_2 per milligram of chlorophyll per hour.

observed. The right trace in Figure 9 shows the difference between transients in inactive centers at pH 8 and 6.5 on a longer time scale. The difference transient which represented the formation/reduction of Y_Z^{ox} decayed with a half-time of about 40 ms (line). This half-time was similar to that observed for the rebinding of the proton that was released in the presence of Y_Z^{ox} (compare Figure 7).

Figure 10 compares the extents of the electrochromic transients due to Y_Z^{ox} in active and inactive centers as a function of the pH. In active material, the extent (about 10 μs after the flash, open circles) was about constant between pH 5.5 and 7.5. At more acidic pH, it decreased concomitantly with the inactivation of the oxygen-evolving capacity (shown as a dashed line in Figure 10). At alkaline pH, the active centers were converted into inactive ones at pH >7.5, probably due to the release of Mn. Consequently, the electrochromism of Y_Z^{ox} in active centers (open circles) dropped to the level which was observed in the impaired material at pH >7.5.

In inactive material, the electrochromism due to Y_Z^{ox} (determined about 150 μs after the flash, open squares) was about constant between pH 9.5 and 8. This amplitude decreased to about zero at pH 6 with an apparent pK of 7.1

(Table 1). This pK was similar to that observed for the decrease of the amplitude of the fast component (k_f) of the oxidation of Y_Z (compare Figure 2B). Below pH 6, the signal extent became negative due to the superimposition of a transient from the equilibrium portion of P_{680}^+ (see Figure 2C and refs *71* and *87*).

In the literature, several electrochromic difference spectra of $Y_Z-Y_Z^{ox}$ can be found that have been obtained with inactive centers from different starting materials at pH ≤7 (*13, 27, 60, 84, 89*). In this pH region, the electrochromism of Y_Z^{ox} was negligible in core particles of the van Leeuwen/Bögershausen type (Figure 10, open squares). We performed the same experiments as with the latter material with a different type of core particles prepared according to Ghanotakis and Lübbers (see Materials and Methods). With oxygen-evolving material, the electrochromism due to Y_Z^{ox} was similar in both core preparations (Figure 10, solid and open circles). In inactive centers, the same pH-dependent decrease of the electrochromic effect of Y_Z^{ox} as in the van Leeuwen/Bögershausen-type cores was observed. Its apparent pK in the Ghanotakis/Lübbers-type core, however, was much lower, 6.1 (Figure 10, solid squares). These differences between the two types of core particles may reflect the different content of extrinsic polypeptides and detergent, possibly causing alterations of the dielectric permittivity at the lumenal side of PSII proteins as previously proposed (*26, 76*).

DISCUSSION

Comparison of the Rates of Electron Transfer from Y_Z to P_{680}^+ in Inactive and Active PSII

The fast component (k_f) of Y_Z oxidation with a half-time of about 1 μs was dominant between pH 7.5 and 10.5 in inactive PSII core particles. Its features were similar to those of the nanosecond components of Y_Z oxidation in oxygen-evolving material (see Table 1, and refs *5* and *70*). The activation energies of these components were low, 0.15 eV (this work) in inactive and ≤0.1 eV in active centers (*90*).

The slowing of the fastest portion of the oxidation of Y_Z from nanoseconds in active centers to about 1 μs in inactive material can likely be explained by the higher activation energy of the electron transfer in the latter case. An increase of the activation energy by 0.1 eV slows the reaction by a

factor of 50. The higher activation energy of electron transfer $Y_Z \rightarrow P_{680}^+$ in inactive centers is in line with a higher polarizability of the more hydrophilic binding pocket of Y_Z (*91*). The latter was also apparent from the about halved amplitudes of the electrochromic shift of the absorption band of P_{680} due to Y_Z^{ox} (see below), and from the halved apparent electrogenicity of electron transfer from Y_Z to P_{680}^+ (*26*).

Both the nanosecond components in active centers and the 1 μs component in inactive ones of electron transfer from Y_Z to P_{680}^+ were pH-independent (between 5.5 and 7.5 in active centers; see refs *64* and *69*), nearly insensitive to H/D isotope substitution (for active material, see this work and refs *42* and *63*), and revealed low activation energies. These features suggest that in both cases the rate of electron transfer was not limited by the transfer of a proton.

The slow component (k_s) of the oxidation of Y_Z appeared in inactive centers at pH <7.5. The redistribution between the fast and slow modes of Y_Z oxidation was described by a titration with an apparent single pK of 7.0. The features of the slow component were very different from those of the fast components. The rate decreased with decreasing pH; the H/D isotope effect was much larger, 2.5, and the activation energy was much higher, 0.3 eV. A counterpart of this slow component may occur in active centers only below pH 4.5 where electron transfer slows from nanoseconds to microseconds (*69*). We believe these features in inactive material indicate the limitation of electron transfer from Y_Z to P_{680}^+ by a proton transfer reaction at pH <7. The pH-dependence of the slow component (k_s) was weak, and the rate decreased only by a factor of about 5 when the pH was lowered from 8 to 4. This pH effect was likely explained by the electrostatic interactions between Y_Z and the proton-transferring groups (see the next paragraph).

The extent of the very slow component (k_v) of P_{680}^+ reduction was increasing at acidic pH. This phase can be assigned to the recombination reaction $Y_Z P_{680}^+ Q_A^- \rightarrow Y_Z P_{680} Q_A$. The overall rate of this process matched at pH 4 the rate constant of the direct recombination that was observed in PSII where Y_Z was mutated to phenylalanine (*92*) or destroyed (*62*). The observed effect is likely explained by a decrease of the equilibrium constant which reflects the ratio between Y_Z^{ox} and P_{680}^+. We attributed this decrease to an increased midpoint potential of the couple Y_Z^{ox}/Y_Z at acidic pH, which is likely caused by the increasing protonation of amino acid residues at the protein boundary. The latter effect likely also accounts for the slowing of the slower component (k_s) of forward electron transfer from Y_Z to P_{680}^+ at acidic pH (see below). The fraction of P_{680}^+ that remained oxidized in equilibrium with Y_Z^{ox} was found to be 50% at a pH of about 4.5; hence, the equilibrium constant at this pH was unity, and the difference between the midpoint potentials of Y_Z and P_{680} was zero. At pH 7.5, only about 10% of P_{680}^+ remained oxidized in equilibrium with Y_Z^{ox}. Thus, ΔE_m was ≤ 0.1 eV at neutral pH. We conclude that the midpoint potential of Y_Z^{ox}/Y_Z increased by about 0.1 eV with respect to the potential of the couple P_{680}^+/P_{680} when the pH was lowered from 7.5 to 4.5. These estimates agree well with previous reports on the difference of the redox potential of P_{680} and Y_Z in Mn-depleted PSII of about 0.1 eV at pH 6.5 (*27, 92*).

Does Y_Z^{ox} Release a Proton into the Bulk?

It has been postulated by various authors (*31, 32, 38−40*) that Y_Z abstracts a hydrogen atom from bound water on each of the four redox transitions of the catalytic cycle of water oxidation. This model implied that the hydroxyl proton of the phenolic moiety of Y_Z was transferred each time to the bulk water of the lumen (*40*).

On one hand, this hypothesis seems to be hard to reconcile with the observations that in oxygen-evolving PSII the extents and rates of proton release vary as function of the S transition, of the pH, and of the preparation (for a review, see ref *41*). Under certain conditions, proton release can be practically absent on transition $S_1 \Rightarrow S_2$ in any PSII preparation (*76*). The variability of the extents has been unequivocally attributed to Bohr effects of peripheral acid groups (*41, 78*). Furthermore, electron transfer from Mn_4X to Y_Z^{ox} shows a negligible H/D isotope effect on some transitions (*42, 63, 93, 94*) which may not be expected if it is steered by the transfer of a hydrogen atom. These results have been discussed in detail elsewhere (*42, 95*).

The present work corroborates the above conclusions. In inactive centers and at alkaline pH, the rate of proton release was the same as in active centers and much lower than the rate of the oxidation of Y_Z. Thus, proton release greatly lagged behind electron transfer. The charge on or near Y_Z^{ox} (see the next section) caused a large local electrochromic effect mainly on the absorption band of P_{680} (*27, 87, 96*). If the proton from Y_Z is released into bulk water, one would expect to observe the concomitant decay of this electrochromism due to the transfer of the positive charge from the low dielectric of the protein into the electrolyte. Such a coupling of the decay of electrochromism with the observable proton release was absent both in inactive centers at alkaline pH (this work) and in active ones (*27, 52, 79*). The electrochromism due to Y_Z^{ox} thus only decayed when the latter was reduced [with half-times that vary as a function of the S transition in active centers (*13, 87*)]. We conclude that in oxygen-evolving centers (between pH 5 and 7.5) and in inactive material at alkaline pH the hydroxyl proton is not transferred into the bulk within the lifetime of Y_Z^{ox} but is trapped inside the protein.

In inactive centers and at acidic pH, the rates of the oxidation of Y_Z and of the observed proton release were about equal. Furthermore, the generation of Y_Z^{ox} did not cause an electrochromic effect. These observations can be understood as follows. Concomitantly with the oxidation of Y_Z by P_{680}^+, the phenolic proton is at least transferred toward the boundary if not directly released into the aqueous bulk phase. This removes the positive net charge as soon as it is formed. Electrochromic transients are therefore absent. The observed proton release is kinetically steered by the oxidation of Y_Z or vice versa. The observed weak pH dependence of the slow component (k_s) may be rationalized by the participation of at least one intermediate group in the proton transfer between Y_Z^{ox} and the boundary (*97*). The increasing protonation of the surface groups with decreasing pH will decrease the pK of this group and gradually slow the deprotonation of Y_Z^{ox}. Perhaps the most important aspect of these results is the experimental demonstration of a behavior where the phenolic proton is removed far away from Y_Z^{ox}. Only this situation would

Scheme 1: Two Hypothetical Models for the Functioning of Tyrosine $Y_Z{}^a$
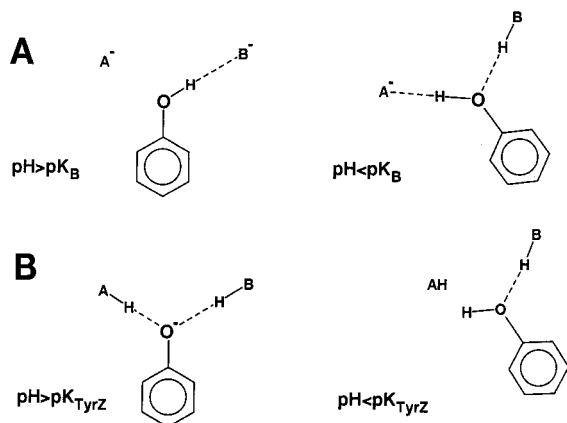
^{a} (A) Y_Z is hydrogen bonded (dashed line) to a base B^- with a pK of 7 in inactive PSII and with a pK of 4.5 in oxygen-evolving PSII. (Left) The transfer of the hydroxyl proton of $Y_Z{}^{ox}$ to B^- is fast and not rate-limiting for electron transfer. (Right) Only when B is protonated the electron abstraction from Y_Z is limited by the transfer of the hydroxyl proton (to a second base A, as shown, or to the bulk water). (B) The pK of Y_Z itself is 7 in inactive centers and 4.5 in oxygen-evolving centers. (Left) These low pK values are in part achieved by modulating hydrogen bonds to the phenol oxygen of $Y_Z{}^-$ from bases A and B. (Right) Electron abstraction from Y_Z is limited by the transfer of the hydroxyl proton (possibly to bulk water) only where pH < pK_{Y_Z} where Y_Z is protonated.

prepare $Y_Z{}^{ox}$ for the postulated function of a hydrogen acceptor (*31, 32, 38−40*). Unfittingly, we found it only in core preparations with inactivated oxygen-evolving capacity and only at acidic pH. This corroborates our view that the phenolic proton of $Y_Z{}^{ox}$ remains in its immediate vicinity in active material. This view is hardly compatible with the postulated hydrogen acceptor function of $Y_Z{}^{ox}$.

Mechanism of the Oxidation of Y_Z

Our results can be rationalized by two related models. Both models are based on the experimental evidence that $Y_Z{}^{ox}$ (*31, 33−36, 98−101*) and $Y_D{}^{ox}$ (*102−105*) are neutral radicals and hydrogen bonded to the CD loops of the D1 and D2 proteins.

Model 1 is shown in Scheme 1A (left). It assumes that Y_Z is neutral (protonated) in the ground state at physiological pH. Upon its oxidation by $P_{680}{}^+$, the pK of the tyrosyl side chain is shifted from presumably 10 to extremely low values (p$K \leq -2$ in water; see ref *77*) and the hydroxyl proton is removed. The low activation energy and the absence of a kinetic H/D isotope effect on the oxidation of Y_Z by $P_{680}{}^+$ implies that the phenolic proton is transferred to a very effective base B^- with a higher rate than that of the electron transfer, i.e. in nanoseconds. The transition is then appropriately denoted as Y_Z-H···$B^- \rightarrow Y_Z{}^{\bullet}···H^+$-$B^-$ (see also refs *42, 70,* and *106*). The positive charge of the proton gives rise to the observed local electrochromic transient. It is likely that the proton is rebound by $Y_Z{}^{ox}$ during its reduction, a proton rocking motion similar to the one that has been proposed to occur upon the oxidoreduction of Y_D (*45*). It should be noted that the rapid release of protons that we observed with pH-indicating dyes does not originate from $Y_Z{}^{ox}$ itself but from electrostatically induced pK shifts of at least three peripheral acid groups with different pK values.

In inactive material, the proton transfer starts to govern the rate of the oxidation of Y_Z if group B is protonated, e.g. below its pK of 7 (Scheme 1A, right). In this case, the proton of $Y_Z{}^{ox}$ is then transferred via a different pathway, e.g. to a different base A (as depicted in Scheme 1A, right) that is closer to the membrane/water interface or to bulk water. The main difference between active and inactive material according to model 1 is that the pK of B is 7 in inactive centers, but 4.5 in active ones. In active material, we expect that electron transfer from Y_Z to $P_{680}{}^+$ is rate-limited by proton transfer only below pH 4.5. Such a limitation has been observed. It is reversible (*68, 69*) unlike the one which is observed at alkaline pH and caused by the loss of Mn from the center.

Model 2 of Y_Z oxidation which is summarized in Scheme 1B differs from model 1 by the assumption that Y_Z is negative ($Y_Z{}^-$, Scheme 1B, left) and electroneutral in its oxidized form, $Y_Z{}^{\bullet}$. The pK values of 7 in inactive PSII and of 4.5 in oxygen-evolving material are then attributed to Y_Z itself. According to model 2, the low activation energy of Y_Z oxidation and the absence of a H/D isotope effect in oxygen-evolving samples (at all studied pH values) and in inactive centers at pH >7 are now simply explained by the absence of any proton transfer upon the oxidation of $Y_Z{}^-$. The oxidation of the tyrosine anion to a neutral tyrosine radical is equivalent to the appearance of a positive charge at the place of Y_Z. This charge causes the observed local electrochromic effect when $Y_Z{}^{ox}$ is present. At pH values lower than the pK of Y_Z (pH <4.5 in oxygen-evolving centers and pH <7 in inactive ones), Y_Z is protonated (Scheme 1B, right). Then, the transfer of the hydroxyl proton (to water or to a nearby base) limits the rate of the electron transfer.

The difficulty of model 2 is the unusually low pK value of Y_Z. The pK of tyrosine is 10 in water, and one expects it to be shifted to even more alkaline values due to the decrease of the Born solvation energy when placed in the low dielectric of a protein (*107*). Still, functional pK values of tyrosine in the range of 6−4.5 have been reported for a family of native and artificial myoglobin mutants (ref *108* and references therein). In the latter case, the pK shift was due to the influence of a heme iron atom. In the case of Y_Z, the anionic state of tyrosine may be stabilized by Mn and Ca atoms in its vicinity. One positive charge spaced by 5 Å from Y_Z may already shift the pK by 3−5 units if we take ϵ in the range of 10−20 (*27*). Another example of a large pK shift is the Q_B-binding site of bacterial reaction centers. The crucial L-Glu212 has an unusual pK of 10 (versus a pK of 4.5 in water) owing to the negative charge on L-Asp213 and to a possible hydrogen bond to the ubiquinone (*109, 110*). A large pK shift of Y_Z may result from the combined action of positive charges on manganese and calcium atoms, and from hydrogen bonds of neighboring amino acids to its phenolic oxygen. Model 2 assumes that the difference between active and inactive materials with respect to Y_Z oxidation is mainly a shift of its pK by about 2.5 units into the alkaline direction (from a pK of 4.5 to 7) due to the loss of the Mn cluster and an increased dielectric polarizability of the protein.

Models 1 and 2 (Scheme 1) cannot be distinguished on the basis of our data alone. They predict, however, that the number and strength of hydrogen bonds to Y_Z may explain the higher midpoint potential and faster oxidation rate of the

latter compared to those of Y_D. These properties likely change as a function of the material (active versus inactive), and of the pH in both the reduced and oxidized states. pH-dependent variations in the ENDOR spectra of Y_Z^{ox} (*111*) suggested a protonation with a similar apparent pK (6−7) in inactive material as reported above. Two hydrogen bonds to Y_Z (as tentatively depicted in Scheme 1) have been observed by the research group of D. Britt (*121*).

Implications on the Structure of PSII and on the Mechanism of Water Oxidation

There is good evidence (*22, 26, 27, 112, 113*) that tyrosines Y_Z and Y_D are placed symmetrically at ∼14 Å from P_{680}, and about 4 Å closer to the lumen. The position of Mn relative to Y_Z and P_{680} is controversial. The Mn cluster has been reported to be in close proximity to [less than 5 Å (*31*)] or at a greater distance from Y_Z [14−20 Å (*27, 30, 114, 115*)], or it may even consist of two Mn dimers (*116*) with a distance of about 10 Å between them (*117*).

The effect of the positive charge stored on Mn during the $S_1 \rightleftharpoons S_2$ transition on the redox equilibrium between Y_Z and P_{680} must be quite different for the above structural arrangements. If the whole tetranuclear Mn cluster would be located at a distance of only 5 Å from Y_Z (as suggested in ref *31*), one positive charge on Mn would raise the redox potential of Y_Z relative to P_{680} by about 180 mV (assuming an effective dielectric constant of 10; see ref *27* and references therein). This would shift the $\Delta G°$ of the equilibrium between Y_Z and P_{680} for the $S_2 \rightleftharpoons S_3$ and $S_3 \rightleftharpoons S_4$ transitions relative to the $S_1 \rightleftharpoons S_2$ transition accordingly. Contrastingly, a rather moderate shift by only about 50 mV was observed (see Results). A distance between a compact tetra-Mn cluster and Y_Z of only 5 Å (as necessary for a hydrogen abstractor function of Y_Z) seems unlikely. It would furthermore be hard to reconcile with the observation of, at the same time, a small activation energy and a relatively low rate ($t_{1/2} \approx 60$ μs) of electron transfer from Mn to Y_Z^{ox} on transition $S_1 \rightleftharpoons S_2$ (*42, 90*). Alternatively, we suggest a triangular arrangement. Either (1) a tetranuclear Mn cluster is located an only slightly smaller distance from Y_Z than from P_{680} (see also ref *27*) or, alternatively, (2) one of the two Mn dimers (*117*), the one which (the auxiliary one) serves to store the positive charge on transition $S_1 \rightleftharpoons S_2$, is placed a similar distance from Y_Z and P_{680}, the other (the catalytic one) is placed closer to Y_Z and participates in water oxidation. In both cases, a positive charge on Mn would increase the oxidizing potentials of both Y_Z and P_{680}. If we take 10−13 and 15−20 Å as estimates of the distances between Mn and Y_Z and Y_Z and P_{680}, respectively, $E_m(Y_Z^{ox}/Y_Z)$ and $E_m(P_{680}^+/P_{680})$ are expected to rise by 125 and 80 mV, respectively, after the $S_1 \rightleftharpoons S_2$ transition (dielectric permittivity of 10). The energy gap between Y_Z and P_{680} then decreases by 45 mV, in line with the observations. The benefit is twofold. (1) The energy gap between these cofactors remains appropriate to assure the sequential electron transfer from Mn via Y_Z to P_{680}^+, and (2) the higher redox potential of P_{680} increases the driving force of the forward reaction (*118*).

Various models have been proposed for the mechanism of water oxidation. Some involve the stepwise oxidation of the substrate during at least some of the lower transitions of the catalytic cycle (*10, 32, 38, 106, 119*), whereas others

pool the abstraction of four electrons from bound water on the final, oxygen-evolving transition $S_4 \rightarrow S_0$ (*42, 120*). Currently discussed models of the first type involve the abstraction of hydrogen atoms from bound water during all four redox transitions of the catalytic cycle (*38, 40*). As argued above, our results in the current work as well as our previous investigations on electron transfer from Mn_4X to Y_Z^{ox} (*42*) make the functioning of Y_Z as a hydrogen abstractor on each step of the catalytic cycle unlikely. Our results are more compatible with a mechanism of water oxidation of the second type. We propose that two sequential two-electron transfer steps with a (bound) peroxide intermediate (see also ref *106*) occur only on transition $S_4 \rightarrow S_0$ and lead to the formation of dioxygen (*42*). In this concept, Y_Z serves two functions: 1) It is an electron transmitter between Mn_4X and P_{680}^+. (2) The effective positive charge that is stored around Y_Z^{ox} in the S_4 state (as $Y_Z^\bullet \cdots H^+-B^-$ derived from $Y_Z-H\cdots B^-$ in model 1, or as $Y_Z^\bullet$ derived from Y_Z^- in model 2) may increase the oxidizing power of the catalytically active Mn by up to 100 mV depending on its distance from Y_Z (see above). During the S_4 to S_0 transition, this increase may be the prerequisite for a shift of the equilibrium between bound water and bound peroxide toward the latter (*42, 106*). Y_Z^{ox}, as an electrostatical promotor, starts the reaction sequence that leads to the production of dioxygen.

CONCLUSIONS

Electron transfer, proton release, and local electrochromism upon the oxidoreduction of the tyrosine, Y_Z, were investigated in inactive and oxygen-evolving PSII core particles under variations of the pH, the temperature, and the H/D isotopic ratio. Only under special conditions (in inactive centers and at acidic pH) is electron transfer from Y_Z to P_{680}^+ steered by the transfer of a proton to the protein/water boundary if not into the bulk. Under all other conditions (active centers in the physiological pH range, inactive centers at alkaline pH), the hydroxyl proton is either trapped by a nearby base inside the protein or intrinsically absent due to the low pK (about 7 in inactive and 4.5 in active centers) of Y_Z. These features make the functioning of Y_Z^{ox} as a hydrogen abstractor from bound water unlikely. Instead, the positive charge on or near Y_Z^{ox} may provide the final oxidizing potential that allows two two-electron abstractions from bound water at the Mn cluster during transition $S_3 \rightleftharpoons S_4 \rightarrow S_0$.

REFERENCES

1. Renger, G. (1988) *Chem. Scr. 28A*, 105−109.
2. Debus, R. J. (1992) *Biochim. Biophys. Acta 1102*, 269−352.
3. Diner, B. A., and Babcock, G. T. (1996) in *Oxygenic photosynthesis: the light reactions* (Ort, D. R., and Yocum, C. F., Eds.) pp 213−247, Kluwer Academic Publishers, Dordrecht, The Netherlands.
4. Schlodder, E., Brettel, K., Schatz, G. H., and Witt, H. T. (1984) *Biochim. Biophys. Acta 765*, 178−185.
5. Brettel, K., Schlodder, E., and Witt, H. T. (1984) *Biochim. Biophys. Acta 766*, 403−415.

6. Barry, B. A., and Babcock, G. T. (1987) *Proc. Natl. Acad. Sci. U.S.A. 84*, 7099−7103.

7. Debus, R. J., Barry, B. A., Babcock, G. T., and McIntosh, L. (1988) *Proc. Natl. Acad. Sci. U.S.A. 85*, 427−430.

8. Barry, B. A. (1995) *Methods Enzymol. 258*, 303−319.

9. Dekker, J. P., Plijter, J. J., Ouwenand, L., and Van Gorkom, H. J. (1984) *Biochim. Biophys. Acta 767*, 176−179.

10. Renger, G., and Wydrzynski, T. (1991) *Biol. Met. 4*, 73−80.

11. Yachandra, V. K., Sauer, K., and Klein, M. P. (1996) *Chem. Rev. 96*, 2927−2950.

12. Styring, S. A., and Rutherford, A. W. (1988) *Biochemistry 27*, 4915−4923.

13. Haumann, M., Drevenstedt, W., Hundelt, M., and Junge, W. (1996) *Biochim. Biophys. Acta 1273*, 237−250.

14. Hundelt, M., Haumann, M., and Junge, W. (1997) *Biochim. Biophys. Acta 1321*, 47−60.

15. Yocum, C. F. (1992) in *Manganese redox enzymes* (Pecoraro, V. L., Ed.) pp 71−83, VCH Publishers, New York.

16. Kok, B., Forbush, B., and McGloin, M. (1970) *Photochem. Photobiol. 11*, 457−475.

17. Hoganson, C. W., and Babcock, G. T. (1989) *Biochemistry 28*, 1448−1454.

18. Rutherford, A. W., Zimmermann, J. L., and Boussac, A. (1992) in *The photosystems: Structure, function and molecular biology* (Barber, J., Ed.) pp 179−229, Elsevier, Amsterdam.

19. Michel, H., and Deisenhofer, J. (1988) *Biochemistry 27*, 1−7.

20. Michel, H., and Deisenhofer, J. (1988) *Appl. Chem. 60*, 953−958.

21. Vermaas, W. F. J., Styring, S., Schröder, W. P., and Andersson, B. (1993) *Photosynth. Res. 38*, 249−263.

22. Svensson, B., Etchebest, C., Tuffery, P., van Kan, P., Smith, J., and Styring, S. (1996) *Biochemistry 35*, 14486−14502.

23. Pokorny, A., Wulf, K., and Trissl, H. W. (1994) *Biochim. Biophys. Acta 1184*, 65−70.

24. Mamedov, M. D., Lovyagina, E. R., Verkhovskii, M. I., Semenov, A. Y., Cherepanov, D. A., and Shinkarev, V. P. (1995) *Biochemistry (Moscow) 59*, 327−341.

25. Haumann, M., Hundelt, M., Drevenstedt, W., and Junge, W. (1995) in *Photosynthesis: from light to biosphere* (Mathis, P., Ed.) pp 333−336, Kluwer Academic Publishers, Dordrecht, The Netherlands.

26. Haumann, M., Mulkidjanian, A. Y., and Junge, W. (1997) *Biochemistry 36*, 9304−9315.

27. Mulkidjanian, A. Y., Cherepanov, D. A., Haumann, M., and Junge, W. (1996) *Biochemistry 35*, 3093−3107.

28. Svensson, B., Vass, I., and Styring, S. (1991) *Z. Naturforsch. 46*, 765−776.

29. Un, S., Brill, T. M., and Zimmermann, J. L. (1994) *Proc. Natl. Acad. Sci. U.S.A. 91*, 5262−5266.

30. Kodera, Y., Hara, H., Astashkin, A. V., Kawamori, A., and Ono, T. (1995) *Biochim. Biophys. Acta 1232*, 43−51.

31. Gilchrist, M. L., Ball, J. A., Randall, D. W., and Britt, R. D. (1995) *Proc. Natl. Acad. Sci. U.S.A. 92*, 9545−9549.

32. Britt, R. D. (1996) in *Oxygenic photosynthesis: The light reactions* (Ort, D., and Yocum, C. F., Eds.) pp 137−164, Kluwer Academic Publishers, Dordrecht, The Netherlands.

33. Mino, H., and Kawamori, A. (1994) *Biochim. Biophys. Acta 1185*, 213−220.

34. Tommos, C., Tang, X. S., Warncke, K., Hoganson, C. W., Styring, S., McCracken, J., Diner, B. A., and Babcock, G. T. (1995) *J. Am. Chem. Soc. 117*, 10325−10335.

35. Force, D. A., Randall, D. W., Britt, R. D., Tang, X. S., and Diner, B. A. (1995) *J. Am. Chem. Soc. 117*, 12643−12644.

36. Tang, X. S., Zheng, M., Chisholm, D. A., Dismukes, G. C., and Diner, B. A. (1996) *Biochemistry 35*, 1475−1484.

37. Warncke, K., Tang, X.-S., Tommos, C., Babcock, G. T., Diner, B. A., and McCracken, J. (1995) in *Photosynthesis: from light to biosphere* (Mathis, P., Ed.) pp 711−715, Kluwer Academic Publishers, Dordrecht, The Netherlands.

38. Babcock, G. T. (1995) in *Photosynthesis: from light to biosphere* (Mathis, P., Ed.) pp 209−215, Kluwer Academic Publishers, Dordrecht, The Netherlands.

39. Hoganson, C. W., Lydakis-Simantiris, N., Tang, X. S., Tommos, C., Warncke, K., Babcock, G. T., Diner, B. A., McCracken, J., and Styring, S. (1995) *Photosynth. Res. 46*, 177−184.

40. Tommos, C., and Babcock, G. T. (1997) *Acc. Chem. Res.* (in press).

41. Haumann, M., and Junge, W. (1996) in *Oxygenic photosynthesis: The light reactions* (Ort, D., and Yocum, C. F., Eds.) pp 165−192, Kluwer Academic Publishers, Dordrecht, The Netherlands.

42. Haumann, M., Bögershausen, O., Cherepanov, D. A., Ahlbrink, R., and Junge, W. (1997) *Photosynth. Res. 51*, 193−208.

43. Haumann, M., and Junge, W. (1994) *Biochemistry 33*, 864−872.

44. Bögershausen, O., and Junge, W. (1995) *Biochim. Biophys. Acta 1230*, 177−185.

45. Babcock, G. T., Barry, B. A., Debus, R. J., Hoganson, C. W., Atamian, M., McIntosh, L., Sithole, U., and Yocum, C. F. (1989) *Biochemistry 28*, 9557−9565.

46. van Leeuwen, P. J., Nieveen, M. C., van de Meent, E. J., Dekker, J. P., and Van Gorkom, H. J. (1991) *Photosynth. Res. 28*, 149−153.

47. Lübbers, K., Haumann, M., and Junge, W. (1993) *Biochim. Biophys. Acta 1183*, 210−214.

48. Cheniae, G. M., and Martin, I. F. (1978) *Biochim. Biophys. Acta 502*, 321−344.

49. Renger, G. (1979) *Biochim. Biophys. Acta 547*, 103−116.

50. Cole, J., Boska, M., Blough, N. V., and Sauer, K. (1986) *Biochim. Biophys. Acta 848*, 41−47.

51. Junge, W. (1976) in *Chemistry and biochemistry of plant pigments* (Goodwin, T. W., Ed.) pp 233−333, Academic Press, London.

52. Haumann, M., Bögershausen, O., and Junge, W. (1994) *FEBS Lett. 355*, 101−105.

53. Renger, G., Eckert, H. J., and Buchwald, H. E. (1978) *FEBS Lett. 90*, 10-ff.

54. Weiss, W., and Renger, G. (1986) *Biochim. Biophys. Acta 850*, 173−183.

55. Doering, G., Renger, G., Vater, J., and Witt, H. T. (1969) *Z. Naturforsch. 24*, 1139−1143.

56. Mathis, P., and Setif, P. (1981) *Isr. J. Chem. 21*, 316−320.

57. Haveman, J., and Mathis, P. (1976) *Biochim. Biophys. Acta 440*, 346−355.

58. Conjeaud, H., and Mathis, P. (1986) *Biophys. J. 49*, 1215−1221.

59. Eckert, H. J., Wiese, N., Bernarding, J., Eichler, H. J., and Renger, G. (1988) *FEBS Lett. 240*, 153−158.

60. Schatz, G. H., and Van Gorkom, H. J. (1985) *Biochim. Biophys. Acta 810*, 283−294.

61. Dekker, J. P., Van Gorkom, H. J., Wensink, J., and Ouwehand, L. (1984) *Biochim. Biophys. Acta 767*, 1−9.

62. Christen, G., Karge, M., Eckert, H. J., and Renger, G. (1997) *Photosynthetica 33*, 529−539.

63. Karge, M., Irrgang, K. D., Sellin, S., Feinaeugle, R., Liu, B., Eckert, H. J., Eichler, H. J., and Renger, G. (1996) *FEBS Lett. 378*, 140−144.

64. Meyer, B., Schlodder, E., Dekker, J. P., and Witt, H. T. (1989) *Biochim. Biophys. Acta 974*, 36−43.

65. van Leeuwen, P. J., Heimann, C., Kleinherenbrink, F. A. M., and Van Gorkom, H. J. (1992) in *Research in photosynthesis* (Murata, N., Ed.) pp 341−344, Kluwer Academic Publishers, Dordrecht, The Netherlands.

66. Lukins, P. B., Post, A., Walker, P. J., and Larkum, A. W. D. (1996) *Photosynth. Res. 49*, 209−221.

67. Witt, H. T., Schlodder, E., Brettel, K., and Saygin, Ö. (1986) *Photosynth. Res. 10*, 453−471.

68. Renger, G., Glaeser, M., and Buchwald, H. E. (1977) *Biochim. Biophys. Acta 461*, 392−402.

69. Schlodder, E., and Meyer, B. (1987) *Biochim. Biophys. Acta 890*, 23−31.

70. Eckert, H. J., and Renger, G. (1988) *FEBS Lett. 236*, 425−431.

71. Rappaport, F., Porter, G., Barber, J., Klug, D. R., and Lavergne, J. (1995) in *Photosynthesis: from light to biosphere II* (Mathis,

P., Ed.) pp 345−348, Kluwer Academic Publishers, Dordrecht, The Netherlands.

72. Förster, V., and Junge, W. (1985) *Photochem. Photobiol. 41*, 183−190.

73. Renger, G., Wacker, U., and Völker, M. (1987) *Photosynth. Res. 13*, 167−184.

74. Wacker, U., Haag, E., and Renger, G. (1990) in *Current research in photosynthesis* (Baltscheffsky, M., Ed.) pp 869−872, Kluwer Academic Publishers, Dordrecht, The Netherlands.

75. Rappaport, F., and Lavergne, J. (1991) *Biochemistry 30*, 10004−10012.

76. Haumann, M., Hundelt, M., Jahns, P., Chroni, S., Bögershausen, O., Ghanotakis, D., and Junge, W. (1997) *FEBS Lett. 410*, 243−248.

77. Land, E. J., Porter, G., and Strachan, E. (1961) *Trans. Faraday Soc. 57*, 1885−1893.

78. Lavergne, J., and Junge, W. (1993) *Photosynth. Res. 38*, 279−296.

79. Kretschmann, H., Schlodder, E., and Witt, H. T. (1996) *Biochim. Biophys. Acta 1274*, 1−8.

80. Förster, V., and Junge, W. (1984) in *Advances in photosynthetic research* (Sybesma, C., Ed.) pp 305−309, Martinus Nijhoff/Dr. W. Junk, The Hague.

81. Renger, G., and Völker, M. (1982) *FEBS Lett. 149*, 203−207.

82. Renger, G., Eckert, H. J., and Völker, M. (1989) *Photosynth. Res. 22*, 247−256.

83. Bell, R. P. (1973) *The proton in chemistry*, Chapman & Hall, London.

84. Dekker, J. P., Van Gorkom, H. J., Brok, M., and Ouwehand, L. (1984) *Biochim. Biophys. Acta 764*, 301−309.

85. Velthuys, B. R. (1988) *Biochim. Biophys. Acta 933*, 249−257.

86. Lavergne, J. (1991) *Biochim. Biophys. Acta 1060*, 175−188.

87. Rappaport, F., Blanchard-Desce, M., and Lavergne, J. (1994) *Biochim. Biophys. Acta 1184*, 178−192.

88. Bögershausen, O., and Junge, W. (1995) in *Photosynthesis: from light to biosphere II* (Mathis, P., Ed.) pp 263−266, Kluwer Academic Publishers, Dordrecht, The Netherlands.

89. Diner, B. A., and de Vitry, C. (1984) in *Advances in photosynthesis* (Sybesma, C., Ed.) pp 407−411, Martinus Nijhoff/Dr. W. Junk, The Hague.

90. Renger, G., Eckert, H. J., Hagemann, R., Hanssum, B., Koike, H., and Wacker, U. (1989) in *Photosynthesis: molecular biology and bioenergetics* (Singhal, G. S., Barber, J., Dilley, R. A., Govindjee, Haselkorn, R., and Mohanty, P., Eds.) pp 357−371, Narosa Publishing House, New Delhi.

91. Yerkes, C. T., Babcock, G. T., and Crofts, A. R. (1983) *FEBS Lett. 158*, 359-ff.

92. Metz, J. G., Nixon, P. J., Rögner, M., Brudvig, G. W., and Diner, B. A. (1989) *Biochemistry 28*, 6960−6969.

93. Renger, G., Bittner, T., and Messinger, J. (1994) *Biochem. Soc. Trans. 22*, 318−322.

94. Lydakis-Simantiris, N., Hoganson, C. W., Ghanotakis, D. F., and Babcock, G. T. (1995) in *Photosynthesis: from light to biosphere II* (Mathis, P., Ed.) pp 279−283, Kluwer Academic Publishers, Dordrecht, The Netherlands.

95. Bögershausen, O., Haumann, M., and Junge, W. (1996) *Ber. Buns. Ges. 100*, 1987−1992.

96. Diner, B. A., Tang, X. S., Zheng, M., Dismukes, G. C., Force, D. A., Randall, D. W., and Britt, R. D. (1995) in *Photosynthesis: from light to biosphere II* (Mathis, P., Ed.) pp 229−234, Kluwer Academic Publishers, Dordrecht, The Netherlands.

97. Mulkidjanian, A. Y., Mamedov, M. D., Semenov, A. Y., Shinkarev, V. P., Verkhovsky, M. I., and Drachev, L. A. (1990) *FEBS Lett. 277*, 127−130.

98. Un, S., Tang, X. S., and Diner, B. A. (1996) *Biochemistry 35*, 679−684.

99. Britt, R. D., Randall, D. W., Ball, J. A., Gilchrist, M. L., Force, D. A., Sturgeon, B. E., Lorigan, G. A., Tang, X. S., Diner, B. A., Klein, M. P., Chan, M. K., and Armstrong, W. H. (1995) in *Photosynthesis: from light to biosphere II* (Mathis, P., Ed.) pp 223−228, Kluwer Academic Publishers, Dordrecht, The Netherlands.

100. MacDonald, G. M., Bixby, K. A., and Barry, B. A. (1993) *Proc. Natl. Acad. Sci. U.S.A. 90*, 11024−11028.

101. Bernard, M. T., MacDonald, G. M., Nguyen, A. P., Debus, R. J., and Barry, B. A. (1995) *J. Biol. Chem. 270*, 1589−1594.

102. Tommos, C., Davidsson, L., Svensson, B., Madsen, C., Vermaas, W. F. J., and Styring, S. (1993) *Biochemistry 32*, 5436−5441.

103. Tang, X. S., Chisholm, D. A., Dismukes, G. C., Brudvig, G. W., and Diner, B. A. (1993) *Biochemistry 32*, 13742−13748.

104. Mino, H., Satoh, J., Kawamori, A., Toriyama, K., and Zimmermann, J. L. (1993) *Biochim. Biophys. Acta 1144*, 426−433.

105. Warncke, K., Babcock, G. T., and McCracken, J. (1994) *J. Am. Chem. Soc. 116*, 7332−7340.

106. Renger, G. (1993) *Photosynth. Res. 38*, 229−247.

107. Warshel, A., and Russell, S. T. (1984) *Q. Rev. Biophys. 17*, 283−422.

108. Pin, S., Alpert, B., Cortes, R., Ascone, I., Chiu, M. L., and Sligar, S. G. (1994) *Biochemistry 33*, 11618−11623.

109. Chang, C.-H., El-Kabbani, Tiede, D., Norris, J., and Schiffer, M. (1991) *Biochemistry 30*, 5352−5360.

110. Gopta, O. A., Bloch, D. A., Cherepanov, D. A., and Mulkidjanian, A. Y. (1997) *FEBS Lett. 412*, 490−494.

111. Mino, H., Astashkin, A. V., Kawamori, A., Ono, T.-a., and Inoue, Y. (1995) in *Photosynthesis: from light to biosphere II* (Mathis, P., Ed.) pp 559−562, Kluwer Academic Publishers, Dordrecht, The Netherlands.

112. Koulougliotis, D., Tang, X. S., Diner, B. A., and Brudvig, G. W. (1995) *Biochemistry 34*, 2850−2856.

113. Ruffle, S. V., Donnelly, D., Blundell, T. L., and Nugent, J. H. A. (1992) *Photosynth. Res. 34*, 287−300.

114. Hoganson, C. W., and Babcock, G. T. (1988) *Biochemistry 27*, 5848−5855.

115. Boussac, A., and Rutherford, A. W. (1992) *Biochemistry 31*, 7441−7445.

116. Renger, G. (1987) *Photosynthetica 21*, 203−224.

117. Smith, P. J., and Pace, R. J. (1996) *Biochim. Biophys. Acta 1275*, 213−220.

118. Krishtalik, L. I. (1986) *J. Electroanal. Chem. 204*, 245−255.

119. Witt, H. T. (1991) *Photosynth. Res. 29*, 55−77.

120. Krishtalik, L. I. (1986) *Biochim. Biophys. Acta 849*, 162−171.

121. Force, D. A., Randall, D. W., and Britt, R. D. (1997) *Biochemistry 36*, 12062−12070.